THE ASTROPHYSICAL JOURNAL, 461:698–712, 1996 April 20

SIMULTANEOUS MULTIWAVELENGTH SPECTRUM AND VARIABILITY OF 3C 279 FROM 10^9 TO 10^{24} Hz

R. C. HARTMAN,[1] J. R. WEBB,[2] A. P. MARSCHER,[3] J. P. TRAVIS,[3] C. D. DERMER,[4] H. D. ALLER,[5] M. F. ALLER,[5] T. J. BALONEK,[6] K. BENNETT,[7] S. D. BLOOM,[3,8] R. FUJIMOTO,[9] W. HERMSEN,[10] P. HUGHES,[5] P. JENKINS,[2] T. KII,[9] J. D. KURFESS,[4] F. MAKINO,[9] J. R. MATTOX,[11] C. VON MONTIGNY,[1,12] T. OHASHI,[13] I. ROBSON,[14] J. RYAN,[15] A. SADUN,[16] V. SCHÖNFELDER,[17] A. G. SMITH,[18] H. TERÄSRANTA,[19] M. TORNIKOSKI,[19] AND M. J. L. TURNER[20]

Received 1995 June 14; accepted 1995 October 26

ABSTRACT

Data from a number of monitoring programs have been combined with data from the *Compton Gamma Ray Observatory* and the *Ginga* X-ray satellite to construct a spectrum covering nearly 15 decades in frequency during or near the time of the 3C 279 γ-ray flare observed by EGRET in 1991 June. A much less complete spectrum is presented for 1991 October. Light curves from early 1991 to mid-1992 are presented for radio, millimeter, submillimeter, infrared, optical, and γ-rays. Although the temporal coverage is incomplete, the only evidence for correlation in variability between the γ-rays and lower frequencies is a flare in the optical R-band that peaks within $\sim$1 day of the maximum in the γ-ray light curve. The variability shows higher relative amplitude in γ-rays than in the R band. We present spectral fits to the overall multi–wave band spectrum averaged over the 1991 June flare corresponding to two models: (i) synchrotron self-Compton (SSC) emission from a relativistic jet and (ii) inverse Compton scattering of seed photons originating external to the jet (ECS) by the synchrotron-emitting relativistic electrons in the jet. Either model can fit the observed spectra satisfactorily. The higher amplitude of the γ-ray variations is as predicted by the SSC model and can be accommodated within the ECS model if the flare is caused by a temporary change in the bulk Lorentz factor of the γ-ray–emitting plasma.

Subject headings: gamma rays: observations — infrared: galaxies — quasars: individual (3C 279) — X-rays: galaxies

1. INTRODUCTION

The detection by the EGRET instrument (Kanbach et al. 1988, 1989; Thompson et al. 1993) on the *Compton Gamma Ray Observatory* of a 1991 June γ-ray flare from the blazar 3C 279 has been reported by Kniffen et al. (1993). A comparable observation during 1991 October 3–17 revealed no significant time variation and a flux level well below the lowest levels observed during the June observation. Low-sensitivity observations during 1991 October 17–31 and 1992 spring resulted in a marginal detection and two upper limits.

The quasar 3C 279 ($z = 0.538$) has been known for some time to be optically violently variable, showing nearly 7 mag of variation (Webb et al. 1990; updated in Fig. 1). It has also been monitored extensively in several radio bands and has shown variability there also, but with generally longer timescales and smaller amplitudes than in the optical (Hughes, Aller, & Aller 1991; Teräsranta et al. 1992). Near-millimeter flares have been observed repeatedly from 3C 279 by Matsuo, Matsumoto, & Murakami (1989) and Stevens et al. (1994).

This object has also been studied extensively in X-rays and exhibited flaring activity in the X-ray band in 1988 (Makino et al. 1989) and again in late 1990 (Makino, Fink, & Clavel 1991). Makino et al. (1990) analyzed the multi-frequency spectrum of 3C 279 during the 1988 flare and found that the millimeter, infrared, and UV fluxes were all correlated and showed substantial correlation with the X-ray flare. The duration of the 1988 X-ray and optical outburst of 3C 279 was several months, compared with the several-day timescale for the 1991 June γ-ray flare.

In this paper, γ-ray data from the EGRET, COMPTEL,

[1] Code 661, NASA/Goddard Space Flight Center, Greenbelt, MD 20771.
[2] Department of Physics, Florida International University, Miami, FL 33199.
[3] Department of Astronomy, Boston University, 725 Commonwealth Avenue, Boston, MA 02215.
[4] Code 7650, Naval Research Laboratory, Washington, DC 20375-5352.
[5] Department of Astronomy, University of Michigan, Ann Arbor, MI 48109.
[6] Department of Physics and Astronomy, Colgate University, Hamilton, NY 13346-1398.
[7] Astrophysics Division, ESTEC/ESA, 2200 AG Noordwijk, The Netherlands.
[8] Asher Space Research Institute, Israel Institute of Technology, Haifa, Israel.
[9] ISAS, 3-1-1, Yoshinodai, Sagamihara, Kanagawa 229, Japan.
[10] SRON-Utrecht, Sorbonnelaan2, 3584 CA Utrecht, The Netherlands.
[11] Astronomy Department, University of Maryland, College Park, MD 20742.
[12] NAS/NRC Resident Research Associate.
[13] Department of Physics, Tokyo Metropolitan University, Minami-Ohsawa 1-1, Hachioji, Tokyo 192-03, Japan.
[14] JCMT, 660 N. Aohoku Place, Hilo, HI 96720.
[15] Institute for Earth, Oceans and Space, University of New Hampshire, Durham, NH 03824.
[16] Bradley Observatory, Agnes Scott College, 141 E. College Avenue, Decatur, GA 30030.
[17] Max-Planck Institüt für Extraterrestrische Physik, D-8046 Garching, Germany.
[18] Department of Astronomy, University of Florida, Gainesville, FL 32611.
[19] Metsähovi Radio Research Station, SF-02540 Kylmala, Finland.
[20] Department of Physics and Astronomy, University of Leicester, Leicester, England.

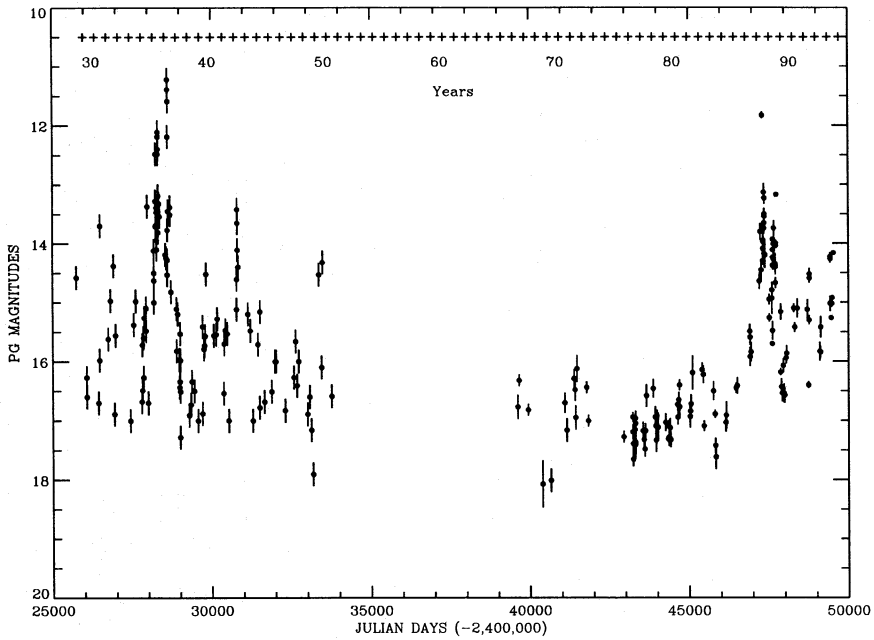

FIG. 1.—Optical light curve of 3C 279 from 1930 to 1994, from the University of Florida monitoring program

and OSSE instruments on the *Compton Gamma Ray Observatory* and X-ray data from the *Ginga* satellite are combined with a wide variety of data obtained via ground-based monitoring in the radio through optical ranges to provide extremely broadband simultaneous spectra for the epochs of the *Compton Gamma Ray Observatory* observations. In addition, light curves of the many frequency bands are presented for an 18 month period starting at the beginning of 1991. We interpret the data using a numerical synchrotron self-Compton model, including shocks in a highly relativistic jet, and an external Compton scattering model. Either model reproduces well the multiwavelength spectra. The multi–waveband characteristics of the 1991 June flare place strong constraints on the models, leading to insights as to the cause of the variability.

2. OBSERVATIONS

2.1. *High-Energy Observations*

The EGRET and COMPTEL γ-ray observations presented here were obtained during five separate *Compton Gamma Ray Observatory* pointings. During 1991 June 16–28 and October 3–17, 3C 279 was about 9° from the EGRET axis, providing high-sensitivity observations of the object. Additional observations were obtained with 3C 279 in low-sensitivity parts of the EGRET field during 1991 October 17–31 and 1992 April 2–16 and April 16–23. The EGRET result shown in this paper for the 1991 October 17–31 observation differs from that presented by Kniffen et al. (1993), based on the same data, because improved analysis software has indicated a high probability that much of the flux assigned to 3C 279 during that interval is due to a nearby transient source (unidentified) which was previously unrecognized. The nearby source had no appreciable effect on the October 3–17 EGRET results.

The October 3–17 observation yielded a γ-ray flux well below that seen in June. The October 17–31 95% confidence upper limit is similar to the October 3–17 flux. 3C 279 was detected at only a 1 σ level during 1992 April 2–16 and was not detected during April 16–23. The photon spectral index was about -1.9 in 1991 June and about -2.1 during the 1991 October 3–17 observation (Kniffen et al. 1993). The difference is significant at roughly a 2 σ level.

The EGRET γ-ray light-curve data are tabulated in Table 1.

The COMPTEL instrument on *CGRO* (Diehl et al. 1992; Schönfelder et al. 1993) also observed 3C 279 during 1991 June 16–28. Although no information is available on temporal variations for that observation, a significant flux was

TABLE 1

EGRET γ-RAY LIGHT CURVE FOR 3C 279

Date	Truncated Julian Date	F[a]	σ
1991 Jun 16	8424	1.38	0.26
1991 Jun 17	8425	1.64	0.28
1991 Jun 18	8426	1.97	0.30
1991 Jun 19	8427	2.69	0.34
1991 Jun 20	8428	2.15	0.31
1991 Jun 21	8429	3.29	0.36
1991 Jun 22	8430	3.86	0.40
1991 Jun 23	8431	3.03	0.42
1991 Jun 24	8432	4.01	0.46
1991 Jun 25	8433	4.49	0.42
1991 Jun 26	8434	2.90	0.38
1991 Jun 27	8435	1.50	0.29
1991 Jun 28	8436	1.02	0.27
1991 Jun 16–28	8423–8436	2.64	0.10
1991 Oct 3–5	8532–8534	0.67	0.21
1991 Oct 5–7	8534–8536	0.67	0.21
1991 Oct 7–9	8536–8538	0.92	0.24
1991 Oct 9–11	8538–8540	0.68	0.22
1991 Oct 11–13	8540–8542	0.98	0.26
1991 Oct 13–15	8542–8544	1.22	0.29
1991 Oct 15–17	8544–8546	0.69	0.30
1991 Oct 03–17	8532–8546	0.87	0.07
1991 Oct 17–31	8546–8560	<0.9	...
1992 Apr 2–9	8714–8721	1.6	1.6
1992 Apr 9–16	8721–8728	<0.5	...

[a] In units of 10^{-6} photons (>100 meV)/(cm^2 s). Upper limits are 95% confidence.

measured in the 8–30 MeV range; for 0.75–8 MeV, only an upper limit was obtained (Williams et al. 1995). Although the 8–30 MeV point is consistent with an extension of the EGRET spectrum, the 0.75–8 MeV upper limit suggests a hardening below 10 MeV. COMPTEL did not detect 3C 279 during the 1991 October or 1992 spring observations; the upper limits during October 3–17 are consistent with an extension of the EGRET spectrum at that time.

Although the OSSE instrument on *CGRO* (Cameron et al. 1992; Johnson et al. 1993) did not observe 3C 279 during 1991 June, an observation was made by OSSE during 1991 September 19–October 3, the 2 weeks just prior to the 1991 October EGRET/COMPTEL observation. The resulting spectral points are given in Table 5.

X-ray observations were obtained with the *Ginga* Large Area Counter (Turner et al. 1989) during the two time intervals 1991 June 17.9–18.2 and 18.8–19.2(UT), near the beginning of the flare observed by EGRET. For each of the two intervals, X-ray spectra were measured in the energy range 1.16–23.2 keV; there is no significant difference between the two spectra. No X-ray observations were possible during the 1991 October *CGRO* observations.

TABLE 2A

R-BAND LIGHT CURVE FOR 3C 279

Date	Truncated Julian Date	m_R	σ_R	Observatory[a]
1991 Feb 14	8302	14.39	0.05	AS(CP)
1991 Mar 21	8336	14.50	0.02	HN[b]
1991 Mar 22	8337	14.50	0.05	HN[b]
1991 Mar 24	8340	14.73	0.05	AS(CP)
1991 Apr 22	8369	13.92	0.05	AS(CP)
1991 May 5	8382	14.15	0.03	HN[b]
1991 May 23.....	8400	14.00	0.02	AS(L)
1991 May 25.....	8402	14.67	0.02	AS(L)
1991 May 26.....	8403	14.52	0.02	AS(L)
1991 May 27.....	8404	14.60	0.02	AS(L)
1991 Jun 5	8413	14.38	0.01	HN[b]
1991 Jun 8	8416	14.39	0.03	TB(FB)
1991 Jun 10.....	8418	14.31	0.02	TB(FB)
1991 Jun 13.....	8420	14.06	0.02	TB(FB)
1991 Jun 21.....	8428	13.62	0.05	TB(FB)
1991 Jun 25.....	8432	13.45	0.05	TB(FB)
1991 Jun 26.....	8433	13.81	0.05	TB(FB)
1991 Jul 1	8438	14.26	0.05	TB(FB)
1991 Jul 4	8441	14.49	0.01	HN[b]
1991 Jul 10.....	8447	14.86	0.05	TB(FB)
1991 Jul 15.....	8452	13.38	0.05	TB(FB)

[a] CP = Capilla Peak, CT = CTIO, F = Foggy Bottom, L = Lowell.
[b] From Netzer et al. 1995.

The 1991 June X-ray spectrum is described by

$$J(E) = (4.0 \pm 0.34) \cdot 10^{-3} E^{-(1.68 \pm 0.05)}$$

photons cm^{-2} s^{-1} keV^{-1},

similar to that seen by *Ginga* in 1987 June (Makino et al. 1989), at which time there was no evidence for flaring activity in 3C 279.

The EGRET, COMPTEL, OSSE and *Ginga* data points used in the multiwavelength spectra are shown in Table 5 along with those for the lower frequencies.

2.2. *Optical and Infrared Observations*

Although no *UBV* data were obtained during the 1991 June EGRET observation, 3C 279 was monitored in *R* band throughout the 1991 May–June–July period until the source was lost to the Sun in late July. The *R*-band data during the γ-ray flare were obtained with the 24 inch (0.60 m) telescope/CCD at the Colgate University Observatory. Additional optical observations (*V*, *R*, *I*) were obtained before and after the γ-flare, at Lowell Observatory with the 42 inch (1.06 m) Hall telescope/CCD and at Capilla Peak with the 24 inch (0.60 m) telescope/CCD, at the Colgate Foggy Bottom Observatory, and at the Wise Observatory with the 1 m telescope/CCD and at the Cerro-Tololo Inter-American Observatory (CTIO). Infrared data (*J*, *H*, *K*, *L'* bands) were obtained at the United Kingdom Infrared Telescope (UKIRT) (Gear et al. 1985). The optical and near-infrared data have been corrected for reddening using the method of Burstein & Heiles (1982) and applying the reddening law of Seaton (1979) using an $E(B-V)$ of 0.01.

Tables 2A–2C list the optical and infrared data used here.

2.3. *Millimeter and Submillimeter Observations*

Observations at 90 GHz (3.3 mm) and 230 GHz (1.3 mm) were made using the Swedish-ESO submillimeter telescope (SEST). Data were also obtained at wavelengths of 350, 450, 800, 1100, 1300, and 2000 μm using the James Clerk Maxwell Telescope (JCMT) at Mauna Kea (Duncan et al. 1990). In order to obtain higher density time sampling at 90 and 230 GHz, the SEST and JCMT observations were augmented by including IRAM observations from Reich et al. (1993).

The submillimeter and millimeter data are shown in Tables 3A–3D.

Observations at 22 and 37 GHz were made at the Metsähovi Radio Research Station. Observations at 4.8, 8.0, and

TABLE 2B

I- AND *V*-BAND DATA FROM 3C 279[a]

Date	Truncated Julian Date	*I* Band		*V* Band		Observatory[b]
		m_I	σ_I	m_V	σ_V	
1991 Feb 14	8301	13.62	0.09	15.01	0.03	CP
1991 Mar 24.....	8339	14.09	0.09	15.36	0.03	CP
1991 Apr 22	8368	13.29	0.09	14.45	0.03	CP
1991 May 23.....	8399	13.44	0.03	15.28	0.03	L
1991 May 25.....	8401	...	...	14.62	0.02	L
1991 May 26.....	8402	...	...	14.66	0.02	L
1991 May 27.....	8403	...	...	14.61	0.02	L

[a] Data from A. Sadun.
[b] CP = Capilla Peak; L = Lowell.

TABLE 2C

UKIRT IR DATA FOR 3C 279[a]

DATE	TRUNCATED JULIAN DATE	*J*		*H*		*K*		*L'*	
		F(mJy)	σ(mJy)	*F*(mJy)	σ(mJy)	*F*(mJy)	σ(mJy)	*F*(mJy)	σ(mJy)
1991 Feb 4.....	8291	12.18	0.61	18.85	0.94	29.70	1.48	61.63	3.08
1991 Mar 6	8321	29.09	1.45	39.68	1.98	57.96	2.90	103.61	5.18
1991 May 26.....	8402	19.67	0.98	28.99	1.45	43.17	2.16	86.26	4.31
1991 Jun 16.....	8423	17.84	0.89	26.34	1.32	39.81	1.99	71.29	3.56
1991 Jul 9	8446	11.26	0.56	17.08	0.85	25.84	1.29	45.60	5.60
1992 Jan 14.....	8635	8.20	0.41	12.53	0.63	19.84	0.99	41.13	2.06
1992 Jan 29	8650	6.20	0.31	10.39	0.52	16.66	0.83	...	...
1992 Apr 28	8740	6.52	0.33	10.32	0.52	16.49	0.82	34.15	1.71

[a] Data from I. Robson.

TABLE 3A

JCMT SUBMILLIMETER DATA FOR 3C 279[a]

DATE	TRUNCATED JULIAN DATE	0.35 mm		0.45 mm		0.8 mm		1.1 mm	
		F(Jy)	σ(Jy)	*F*(Jy)	σ(Jy)	*F*(Jy)	σ(Jy)	*F*(Jy)	σ(Jy)
1991 Feb 15	8302	...	...	6.10	0.20	10.80	0.54	12.70	0.64
1991 Apr 8.....	8354	4.70	0.90	6.10	0.40	10.30	0.50	13.60	0.20
1991 Apr 20	8366	...	...	...	...	10.00	0.80	11.71	0.80
1991 May 17.....	8393	3.47	1.12	4.76	0.71	7.68	0.38	9.41	0.47
1991 Jun 10.....	8417	...	...	3.84	0.70	7.13	0.40	8.48	0.40
1991 Jul 17.....	8454	...	...	...	...	7.62	0.40	8.80	0.30
1991 Aug 25	8493	...	...	...	...	8.20	1.00	10.80	0.54
1991 Sep 15.....	8514	...	...	...	...	3.58	0.50	6.35	1.00
1991 Oct 30.....	8559	...	...	...	...	7.89	0.10	10.08	0.10
1991 Nov 29	8589	...	...	...	...	8.10	1.00	9.03	0.30

[a] Data from I. Robson.

TABLE 3B

230 GHz LIGHT CURVE FOR 3C 279

Date	Truncated Julian Date	*F*(Jy)	σ(Jy)	Observatory[a]
1991 Jan 11	8267	17.85	1.87	I
1991 Feb 23	8310	11.95	1.79	I
1991 Feb 27	8314	11.34	1.14	I
1991 Apr 5.....	8351	15.58	1.00	S
1991 Apr 8.....	8354	12.90	0.13	J
1991 Apr 12	8358	16.56	2.07	I
1991 Apr 20	8366	13.44	1.00	J
1991 May 17.....	8393	10.28	0.51	J
1991 Jun 10.....	8417	8.69	0.40	J
1991 Jun 11.....	8418	13.64	1.33	I
1991 Jun 14.....	8421	9.93	1.01	I
1991 Jul 4.....	8441	7.05	0.65	S
1991 Jul 17.....	8454	9.15	0.30	J
1991 Aug 25	8493	11.50	0.60	J
1991 Sep 15.....	8514	7.03	1.20	J
1991 Oct 30.....	8559	10.27	0.10	J
1991 Nov 29	8589	9.40	0.30	J
1991 Dec 3.....	8593	12.30	2.00	I
1992 Jan 7	8628	8.66	0.87	I
1992 Feb 20	8672	6.34	0.75	I
1992 Mar 4	8685	7.79	0.80	I
1992 Mar 9	8690	7.45	0.81	I
1992 Mar 11	8692	6.86	0.74	I

[a] I = IRAM (H. Steppe); J = JCMT (I. Robson); S = SEST (M. Tornikoski).

TABLE 3C

150 GHz LIGHT CURVE FOR 3C 279

Date	Truncated Julian Date	*S*(Jy)	σ(Jy)	Observatory[a]
1991 Apr 8.....	8354	16.30	0.40	J
1991 Apr 12	8358	17.39	1.76	I
1991 Apr 20	8366	14.58	1.10	J
1991 May 17.....	8393	13.20	0.66	J
1991 Jun 10.....	8417	11.51	0.60	J
1991 Jul 17.....	8454	12.06	0.50	J
1991 Jul 25.....	8462	12.57	1.55	I
1991 Aug 25	8493	13.70	0.60	J
1991 Sep 3	8502	17.04	1.74	I
1991 Sep 15.....	8514	11.30	1.50	J
1991 Oct 30.....	8559	13.09	0.16	J
1991 Nov 29	8589	13.77	0.50	J
1992 Jan 29	8650	9.74	1.88	I
1992 May 12.....	8754	7.02	0.73	I
1992 May 29.....	8771	10.86	1.09	I

[a] I = IRAM (H. Steppe); J = JCMT (I. Robson); S = SEST (M. Tornikoski).

TABLE 3D

90 GHz LIGHT CURVE FOR 3C 279

Date	UT (hr:min)	Truncated Julian Date	F (Jy)	σ (Jy)	Observatory[a]
1991 Jan 11	...	8267.5	22.59	1.17	I
1991 Jan 22	...	8278.5	20.58	1.03	I
1991 Feb 27	6:15	8313.26	24.50	1.09	S
1991 Mar 19	...	8334.5	16.27	0.85	I
1991 Apr 2	...	8348.5	19.37	1.04	I
1991 Apr 5.....	4:00	8352.17	21.96	0.94	S
1991 Apr 23	...	8369.5	18.57	0.96	I
1991 May 11....	...	8387.5	20.72	1.04	I
1991 May 12....	...	8388.5	18.62	0.96	I
1991 May 29....	...	8405.5	18.83	1.42	I
1991 May 31....	...	8407.5	15.61	0.86	I
1991 Jun 11.....	...	8418.5	15.6	0.79	I
1991 Jun 14.....	...	8421.5	15.65	0.78	I
1991 Jun 23.....	0:55	8431.04	15.66	0.72	S
1991 Jul 19.....	0:10	8457.01	14.89	0.69	S
1991 Jul 25.....	...	8462.5	15.15	0.76	I
1991 Aug 2	23:40	8471.99	15.85	0.73	S
1991 Sep 3	...	8504.5	19.49	0.98	I
1991 Sep 23.....	...	8522.5	14.64	0.85	I
1991 Dec 1.....	10:25	8592.43	14.02	0.61	S
1991 Dec 3.....	...	8593.5	15.70	0.79	I
1991 Dec 8.....	...	8598.5	15.12	1.44	I
1991 Dec 24	9:00	8615.38	14.09	0.60	S
1991 Dec 25	9:00	8616.38	13.93	0.62	S
1992 Jan 5	...	8626.5	16.02	0.84	I
1992 Jan 7	...	8628.6	15.31	0.77	I
1992 Jan 14.....	...	8635.5	14.71	1.29	I
1992 Jan 28.....	...	8649.5	15.75	0.81	I
1992 Feb 4.....	...	8656.5	15.05	0.75	I
1992 Feb 12	8:35	8664.36	13.88	0.62	S
1992 Feb 13	8:05	8665.34	13.23	0.59	S
1992 Mar 19	...	8700.5	14.48	0.72	I
1992 Apr 14	5:05	8727.21	12.49	0.54	S
1992 Apr 22	...	8734.5	13.04	0.65	I
1992 May 12....	...	8754.5	13.44	0.68	I
1992 May 26....	19:05	8769.80	9.11	0.71	M
1992 May 29....	...	8771.5	14.52	0.73	I

[a] I = IRAM; M = Metsähovi (87 GHz); S = SEST.

14.5 GHz of flux density and polarization were made with the University of Michigan's 26 m paraboloid telescope.

The radio data are listed in Tables 4A–4E.

2.4. *Ultraviolet Data*

There were no UV data obtained for 3C 279 near the time of the 1991 June γ-ray flare. In order to provide a rough estimate of the UV level, however, the 4 yr Bonnell, Vestrand, & Stacy (1994) compilation of *IUE* observations of 3C 279 has been used to estimate its likely UV flux during 1991 June. During that 4 yr period, three *IUE* spectra were made nearly simultaneous with *R*-Band observations. They show an apparent strong correlation between the UV and *R*-band fluxes (although the availability of only three simultaneous *IUE*/*R* observation pairs dictates considerable caution). On 1989 June 8 (one of the three *R*-band measurements simultaneous with *IUE* observations), the *R*-band magnitude (13.61) was almost identical with that taken during 1991 June. In light of the apparent strong *R*/UV correlation, we have used the corresponding 1989 June 8 *IUE* spectra as estimates of the UV in our 1991 June multiwavelength spectrum. Where these values have been used in Figure 5 below, their symbols are distinctly different from those for the simultaneous observations.

3. RESULTS

3.1. *Multifrequency Variability*

Figures 2*a*–2*f* show the temporal behavior in each frequency band from early 1991 to mid-1992; in order to emphasize the relative magnitudes of the variations in the different bands, the vertical logarithmic scale is the same in each subplot. To demonstrate more clearly the variations in the 4.8–90 GHz range, Figure 3 shows those data with a magnified vertical scale; also shown in Figure 3 are the time histories of the polarization and its position angle in the 4.8, 8.0, and 14.5 GHz emissions.

Within each of the optical, infrared, and submillimeter subplots of Figures 2*c*–2*e*, the various bands are consistent in their time variation patterns where they can be compared. There is less correspondence between the subplots, however. The infrared and millimeter-submillimeter regions both show a general decrease in flux over the 18 months covered, but the details of shorter term variations cannot in general be compared.

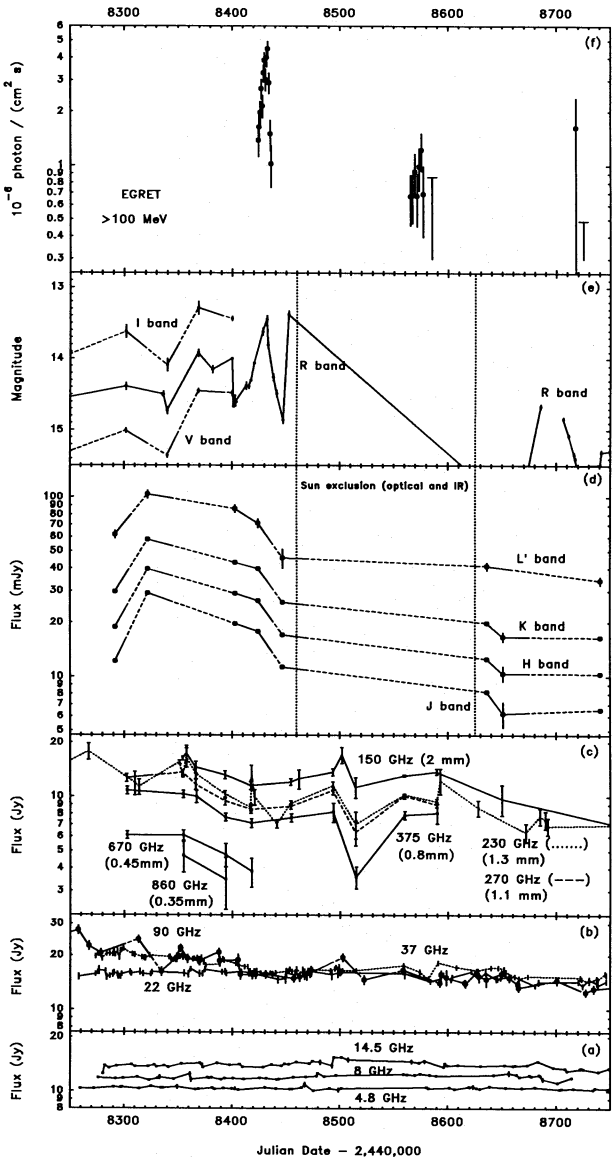

FIG. 2.—Multifrequency light curves for 3C 279 from 1991.0 to 1992.5. To permit comparison of variation amplitudes, the logarithmic vertical scales are chosen to be the same in each subplot.

TABLE 4A

37 GHz LIGHT CURVE FOR 3C 279

Date	UT (hr:min)	Truncated Julian Date	F(Jy)	σ(Jy)	Date	UT (hr:min)	Truncated Julian Date	F(Jy)	σ(Jy)
1991 Jan 17	2:45	8274.11	19.74	0.53	1991 Jun 18	17:20	8426.72	15.94	0.41
1991 Jan 19	2:40	8276.11	20.43	0.55	1991 Jun 27	17:10	8435.72	15.95	0.41
1991 Jan 20	3:45	8277.16	20.33	0.53	1991 Jun 29	17:35	8437.73	15.78	0.43
1991 Jan 23	2:55	8280.12	19.18	0.52	1991 Jul 2	17:30	8440.73	15.97	0.43
1991 Jan 27	2:40	8284.11	20.33	0.51	1991 Jul 14	16:05	8452.67	16.35	0.44
1991 Jan 30	2:40	8287.11	20.42	0.54	1991 Jul 15	16:25	8453.68	16.74	0.45
1991 Feb 2	2:20	8288.10	20.30	0.56	1991 Jul 17	16:45	8455.70	16.23	0.48
1991 Feb 3	2:10	8289.09	21.45	0.55	1991 Jul 22	15:30	8460.00	16.72	0.63
1991 Feb 4	2:25	8290.10	20.23	0.53	1991 Jul 28	16:00	8466.67	15.70	0.44
1991 Feb 6	1:40	8292.07	21.10	0.57	1991 Aug 1	15:05	8470.63	16.55	0.44
1991 Feb 8	2:25	8294.10	19.37	0.54	1991 Aug 3	14:45	8472.61	16.57	0.43
1991 Feb 9	1:20	8295.06	21.23	0.57	1991 Aug 5	14:05	8474.59	16.64	0.44
1991 Feb 10	3:05	8296.13	21.49	0.57	1991 Aug 22	14:40	8491.61	16.44	0.46
1991 Feb 12	1:30	8298.06	21.73	0.57	1991 Aug 26	13:10	8495.55	16.84	0.45
1991 Feb 20	2:05	8306.09	20.27	0.55	1991 Aug 27	12:15	8496.51	17.22	0.46
1991 Feb 22	2:50	8308.12	20.20	0.58	1991 Aug 30	13:05	8499.55	17.41	0.46
1991 Mar 1	0:55	8317.04	19.54	0.52	1991 Sep 1	13:20	8501.56	16.19	0.45
1991 Mar 3	1:50	8319.08	19.38	0.54	1991 Sep 2	13:10	8502.55	16.46	0.45
1991 Mar 4	1:00	8320.04	19.32	0.62	1991 Sep 15	12:10	8515.51	16.44	0.45
1991 Mar 8	0:40	8324.03	20.01	0.52	1991 Oct 29	8:55	8559.37	17.60	0.48
1991 Mar 25	22:20	8341.93	19.54	0.52	1991 Nov 13	8:20	8574.35	16.25	0.48
1991 Mar 26	23:15	8342.97	19.68	0.52	1991 Nov 21	8:50	8582.37	14.81	0.47
1991 Mar 27	22:55	8343.95	19.12	0.50	1991 Nov 30	6:35	8591.27	18.27	0.48
1991 Mar 29	22:30	8345.94	18.92	0.49	1991 Dec 17	4:50	8608.20	17.22	0.46
1991 Mar 31	23:25	8348.00	18.85	0.52	1992 Jan 6	5:20	8628.22	16.44	0.50
1991 Apr 1	22:45	8348.95	19.43	0.50	1992 Jan 18	3:45	8640.16	17.11	0.45
1991 Apr 4	22:25	8351.93	19.65	0.60	1992 Jan 25	2:35	8647.11	17.08	0.47
1991 Apr 6	22:05	8353.92	19.95	0.52	1992 Jan 30	2:15	8652.09	16.88	0.45
1991 Apr 7	21:20	8354.89	19.48	0.55	1992 Jan 31	3:25	8653.14	15.91	0.42
1991 Apr 16	22:15	8363.93	19.07	0.50	1992 Feb 1	2:55	8653.12	16.21	0.43
1991 Apr 17	22:20	8364.93	19.20	0.51	1992 Feb 13	2:50	8665.12	14.86	0.43
1991 Apr 20	21:50	8367.91	19.37	0.50	1992 Feb 21	2:05	8673.09	15.33	0.41
1991 Apr 21	23:50	8368.99	18.66	0.63	1992 Apr 9	21:45	8722.91	15.06	0.40
1991 Apr 23	21:00	8370.88	18.96	0.49	1992 Apr 10	22:20	8723.93	14.81	0.39
1991 Apr 24	21:00	8371.88	19.45	0.50	1992 Apr 17	22:30	8730.94	14.30	0.39
1991 Apr 26	22:05	8373.92	18.33	0.50	1992 Apr 24	20:20	8737.85	14.96	0.39
1991 Apr 28	21:35	8375.90	17.62	0.51	1992 Apr 25	21:35	8738.90	14.71	0.39
1991 May 11	20:05	8388.84	17.87	0.46	1992 May 2	20:25	8745.85	15.89	0.42
1991 May 14	20:00	8391.83	19.04	0.50	1992 May 3	19:15	8746.80	15.62	0.43
1991 May 15	18:50	8392.78	18.77	0.50	1992 May 31	19:20	8774.81	14.72	0.40
1991 May 26	18:30	8403.77	18.03	0.49	1992 Jun 1	18:55	8775.79	15.46	0.42
1991 Jun 3	19:15	8411.80	17.24	0.46	1992 Jun 2	19:10	8776.80	15.24	0.41
1991 Jun 6	18:30	8414.77	17.31	0.45	1992 Jun 4	18:50	8778.78	14.88	0.40
1991 Jun 8	20:30	8416.85	16.28	0.54	1992 Jun 5	19:35	8779.82	14.00	0.41
1991 Jun 12	17:10	8420.72	16.25	0.43	1992 Jun 6	19:05	8780.80	14.22	0.39
1991 Jun 14	18:30	8422.77	16.45	0.44	1992 Jun 7	17:55	8781.75	15.37	0.45

During the early portion of 1991, the radio spectrum peaked around 90 GHz. During the first 5 months of 1991, the 90 GHz flux decreased rather steadily, the decay of a sharp spike which peaked near the beginning of 1991. Largely due to the 90 GHz decrease, the 22–90 GHz spectrum gradually flattened, attaining a spectral index near zero in 1991 June and thereafter attaining a negative exponent. Thus, the peak of the spectrum changed from about 90 GHz to about 30 GHz, with the transition occurring around the time of the 1991 June γ-ray flare. The 90 GHz flux density also stopped decreasing about that time.

The higher frequencies were not as well sampled as the radio. At the time of the 1991 June γ-ray flare, the millimeter and submillimeter fluxes appear to have been in a broad minimum, and the infrared fluxes were beginning an apparent smooth decrease which shortly thereafter became more rapid. In the optical bands, only the R-band data cover the time of the γ-ray flare; during the earlier time when V- and I-band observations were also available, the variations in the three bands were well correlated.

Since correlations between time variations in various frequency bands, along with the corresponding time delays in those variations, appear to represent a promising approach for choosing between various models for the continuum emission of such objects as 3C 279 (e.g., Marscher & Bloom 1994), the appearance of a sharp peak in the R-band flux, with maximum brightness at the same time as the peak of the γ-ray flare, is extremely intriguing. Figure 4 shows a magnification of the γ and optical outbursts. If this represents a real correlation, it would tend to support a model which predicts near-zero time lag between the optical and γ-ray correlated variations, such as synchrotron self-Compton or external Compton scattering models. The simultaneous variations would be fortuitous in inhomogeneous models in which the spectrum is formed by a superposition of separately emitting components.

TABLE 4B

22 GHz Light Curve for 3C 279

Date	UT (hr:min)	Truncated Julian Date	F (Jy)	σ (Jy)	Date	UT (hr:min)	Truncated Julian Date	F (Jy)	σ (Jy)
1991 Jan 1	5:20	8258.22	15.19	0.62	1991 Jul 12.....	15:35	8450.65	16.00	0.88
1991 Jan 17	3:35	8274.15	15.73	0.45	1991 Jul 20.....	15:50	8458.66	15.55	0.84
1991 Jan 19	3:10	8276.13	16.15	0.45	1991 Jul 27.....	16:05	8465.67	16.20	0.99
1991 Jan 20	4:30	8277.19	16.50	0.77	1991 Jul 29.....	16:35	8467.69	15.77	1.02
1991 Jan 26	3:40	8283.15	16.32	0.48	1991 Jul 31.....	15:25	8469.64	15.43	0.82
1991 Jan 27	3:30	8284.15	15.15	0.53	1991 Aug 4.....	14:15	8473.59	16.33	1.05
1991 Jan 30	3:30	8287.15	15.37	0.43	1991 Aug 23	14:30	8492.60	15.67	0.91
1991 Feb 2.....	1:25	8288.06	15.75	0.56	1991 Aug 29	13:55	8498.58	16.00	0.87
1991 Feb 3.....	2:55	8289.12	16.00	0.44	1991 Aug 31	12:35	8500.52	16.13	0.68
1991 Feb 6.....	2:25	8292.10	15.70	0.46	1991 Oct 30.....	8:45	8560.36	15.95	0.97
1991 Feb 7.....	2:25	8293.10	15.29	0.50	1991 Nov 23	6:45	8584.28	14.37	0.43
1991 Feb 8.....	1:20	8294.06	15.30	0.42	1991 Dec 2.....	7:05	8593.30	14.89	0.46
1991 Feb 9.....	2:40	8295.11	15.24	0.44	1991 Dec 3.....	6:30	8594.27	14.84	0.40
1991 Feb 10	2:10	8296.09	15.73	0.43	1991 Dec 5.....	6:35	8596.27	15.64	0.46
1991 Feb 18	1:15	8304.05	16.17	0.45	1991 Dec 12	5:15	8603.22	14.65	0.43
1991 Feb 19	1:35	8305.07	15.84	0.42	1991 Dec 13	5:35	8604.23	15.15	0.46
1991 Feb 27	1:15	8313.05	16.19	0.61	1991 Dec 31	4:55	8622.20	16.28	0.45
1991 Mar 2	1:05	8318.05	15.80	0.51	1992 Jan 7	3:40	8629.15	14.74	0.48
1991 Mar 9	0:10	8325.01	15.73	0.42	1992 Jan 13	4:10	8635.17	16.09	0.53
1991 Mar 10.....	0:55	8326.04	16.16	0.43	1992 Jan 23	3:00	8645.13	14.79	0.46
1991 Apr 8.....	21:30	8355.90	15.92	0.56	1992 Jan 24	3:35	8646.15	14.76	0.42
1991 Apr 12	23:45	8359.99	15.72	0.61	1992 Jan 27	2:55	8649.12	15.02	0.41
1991 Apr 14	20:55	8361.87	16.77	0.48	1992 Feb 9.....	2:55	8661.12	15.30	0.43
1991 Apr 22	21:40	8369.90	15.82	0.55	1992 Feb 28	1:25	8680.06	13.61	0.38
1991 Apr 25	21:05	8372.88	15.81	0.48	1992 Mar 2	0:15	8684.01	14.22	0.52
1991 Apr 27	21:35	8374.90	16.68	0.54	1992 Apr 7.....	22:20	8720.93	14.32	0.41
1991 May 13.....	19:10	8390.80	16.15	0.49	1992 Apr 11	21:30	8724.90	13.53	0.40
1991 May 16.....	18:40	8393.78	16.24	0.55	1992 Apr 17	21:40	8730.90	14.72	0.47
1991 May 31.....	18:40	8408.78	16.22	0.51	1992 Apr 24	21:05	8737.88	14.06	0.41
1991 May 17.....	20:15	8394.84	15.92	0.51	1992 Apr 25	22:15	8738.93	13.61	0.44
1991 Jun 7	17:45	8415.74	15.99	0.69	1992 May 3.....	19:55	8746.83	14.35	0.43
1991 Jul 4.....	16:00	8442.67	14.72	0.67	1992 Jun 7	18:35	8781.77	13.81	0.71
1991 Jul 11.....	17:25	8449.73	14.83	0.83					

If the R-band time sampling were as sparse as that in the infrared, submillimeter, and millimeter bands, its light curve would not look greatly different from the histories obtained for those bands; the peak coincident with the γ-ray flare would tend to disappear. Thus, the lack of observed time structure in the infrared and submillimeter bands might be attributed just to undersampling. This highlights the importance of frequent monitoring observations.

3.2. *Multifrequency Spectra*

A multifrequency F_ν spectrum for the 1991 June period, covering nearly 15 decades in frequency, is presented in Figure 5*a*. Also included are the less numerous observations available during or around the 1991 October *CGRO* observation. Although substantial γ-ray variation was observed by EGRET during the June period, the 13 day average of the γ-ray spectrum has been plotted. This average level corresponds roughly to that at the time of the X-ray observations. The R-band optical data were also averaged over the flare for use in Figure 5.

The *IUE* results, scaled as described above (shown as open squares), serve to bridge partially the large gap in frequency coverage between the optical and the X-ray bands. Unfortunately, the UV/X-ray gap is still substantial, as is that between the submillimeter and infrared observations.

The observed energy content in each spectral band is shown most easily in a νF_ν plot, which is shown in Figure 5*b* for the 1991 June 16–28 epoch. As noted previously by Hartman et al. (1992), the γ-rays dominate the *detected* energy from 3C 279 during that time period; the frequency distribution in energy *output*, however, depends upon the (unknown) relative beaming factors in the various frequency bands. A naive interpolation and integration over the 1991 June spectrum gives an apparent bolometric luminosity (in the reference frame defined by the redshift) of 5.6×10^{48} ergs s^{-1}, of which 3×10^{48} ergs s^{-1} is between 10^{21} and 10^{24} Hz, the γ-ray range.

Table 5 shows the values plotted in Figure 5. Note that, for the 1991 September–October spectrum, the time periods of the OSSE and EGRET observations do not overlap but are contiguous. Also, due to Sun constraints, there were no ground-based observations simultaneous with the 1991 October EGRET observation; the points listed and plotted are averages of measurements taken before and after the EGRET observations, for the frequencies which showed little difference between the before and after measurements. This was not done for frequencies above about 250 GHz because the before/after differences appear to be substantially greater than the observational errors.

For comparison with multiwavelength spectra from earlier quiescent and active periods, points are included from 1984 (Brown et al. 1989) and 1988 March–July (Makino et al. 1989).

4. INTERPRETATION

4.1. *Background*

A rather wide variety of scenarios has been proposed to explain the large apparent γ-ray luminosity of 3C 279 and

TABLE 4C

14.5 GHz Light Curve for 3C 279

Date	UT (hr)	Truncated Julian Date	F (Jy)	σ (Jy)	Polarization (%)	σ (%)	Position Angle	σ
1991 Jan 23	9.46	8280.39	12.50	0.12	4.37	0.56	79°09	4°47
1991 Jan 25	9.71	8282.40	13.82	0.21	3.13	0.14	87.88	1.27
1991 Jan 29	7.85	8286.33	13.43	0.11	3.66	0.16	87.77	1.10
1991 Feb 7	8.83	8293.37	13.75	0.20	3.39	0.16	85.88	1.29
1991 Feb 21	7.82	8307.33	14.03	0.27	3.35	0.18	80.44	2.11
1991 Feb 24	6.23	8310.26	13.73	0.23	3.79	0.33	77.80	2.54
1991 Mar 6	7.91	8322.33	13.69	0.13	3.61	0.53	76.04	3.60
1991 Mar 12	6.93	8328.29	13.94	0.20	3.61	0.14	74.61	1.10
1991 Mar 14	7.36	8330.31	13.62	0.14	3.69	0.15	73.94	1.18
1991 Mar 21	6.79	8337.28	13.86	0.15	3.22	0.27	74.73	2.69
1991 Mar 25	4.02	8341.17	13.59	0.11	3.88	0.23	75.92	1.33
1991 Apr 6	5.51	8353.23	14.15	0.14	2.87	0.14	73.92	1.39
1991 Apr 23	4.07	8370.17	14.28	0.18	1.99	0.18	77.57	2.53
1991 Apr 25	4.45	8372.19	14.08	0.16	1.80	0.14	78.92	2.23
1991 Apr 26	1.71	8373.07	13.55	0.15	2.50	0.14	79.86	1.56
1991 May 9	4.08	8386.17	14.31	0.23	1.78	0.53	72.02	9.20
1991 May 21	2.84	8398.12	13.97	0.14	1.08	0.14	77.11	3.58
1991 May 30	2.42	8407.10	14.13	0.11	0.31	0.23	84.54	30.03
1991 Jun 1	23.82	8409.99	13.65	0.10	0.86	0.16	72.60	5.87
1991 Jun 21	1.03	8429.04	13.59	0.10	0.76	0.13	50.33	5.10
1991 Jun 29	0.18	8437.01	14.02	0.12	0.96	0.17	31.03	5.62
1991 Jul 7	23.15	8445.96	13.80	0.26	1.10	0.18	33.78	3.95
1991 Jul 10	22.92	8448.96	14.20	0.15	1.08	0.15	37.67	3.54
1991 Jul 14	20.98	8452.87	14.14	0.10	1.15	0.17	50.36	3.60
1991 Jul 21	23.09	8459.96	14.53	0.20	1.21	0.20	27.97	4.43
1991 Aug 2	21.70	8471.90	14.23	0.26	1.58	0.15	32.06	2.92
1991 Aug 5	19.01	8474.79	14.66	0.13	1.13	0.14	43.00	3.66
1991 Aug 12	21.03	8481.88	14.50	0.38	0.90	0.17	28.90	5.35
1991 Aug 23	20.12	8492.84	13.87	0.37	1.23	0.18	34.02	4.22
1991 Aug 25	20.32	8494.85	15.40	0.11	1.42	0.16	33.36	3.55
1991 Sep 1	19.72	8501.82	15.42	0.13	1.67	0.21	38.95	2.98
1991 Sep 7	17.32	8507.72	14.97	0.35	1.76	0.25	32.67	3.77
1991 Nov 5	14.55	8566.61	14.64	0.33	1.48	0.21	58.25	4.29
1991 Nov 12	14.69	8573.61	14.39	0.16	2.13	0.25	54.65	3.40
1991 Nov 17	13.88	8578.58	14.73	0.31	1.91	0.15	51.62	2.07
1991 Dec 5	11.51	8596.48	13.61	0.23	2.08	0.15	54.24	1.92
1991 Dec 6	13.85	8597.58	14.24	0.30	2.00	0.15	36.89	2.03
1991 Dec 8	13.51	8599.56	13.90	0.19	2.00	0.15	42.14	2.07
1991 Dec 18	12.89	8609.54	13.99	0.19	1.87	0.19	58.19	2.79
1992 Jan 8	10.92	8630.45	13.85	0.15	1.73	0.17	63.17	2.57
1992 Jan 30	8.76	8652.37	13.99	0.18	1.99	0.14	63.80	2.04
1992 Feb 8	9.48	8660.40	13.82	0.18	1.73	0.15	68.50	2.50
1992 Feb 10	7.20	8662.30	13.88	0.24	2.09	0.22	72.63	2.65
1992 Feb 21	8.78	8673.37	13.97	0.09	1.90	0.24	58.42	3.50
1992 Mar 1	8.07	8683.34	14.64	0.20	2.52	0.29	58.63	3.23
1992 Mar 15	7.39	8697.31	13.54	0.23	2.17	0.15	60.95	2.03
1992 Mar 26	7.10	8708.30	13.38	0.11	2.05	0.16	64.79	2.24
1992 Mar 28	3.53	8710.15	12.96	0.15	2.45	0.18	71.26	2.09
1992 Apr 9	4.29	8722.18	13.27	0.13	1.91	0.18	64.61	2.79
1992 Apr 10	5.05	8723.21	13.43	0.13	1.56	0.14	69.98	2.49
1992 Apr 12	4.95	8725.21	13.29	0.09	1.53	0.18	66.14	3.38
1992 Apr 26	4.05	8739.17	12.88	0.11	1.94	0.25	66.31	3.70
1992 May 6	2.96	8749.12	13.46	0.19	1.82	0.14	70.53	2.19
1992 May 8	3.22	8751.13	13.42	0.13	2.00	0.14	68.88	2.02
1992 May 17	3.06	8760.13	13.25	0.18	2.03	0.14	72.93	1.97
1992 May 28	1.89	8771.08	13.47	0.09	2.16	0.14	71.95	1.81
1992 May 30	1.72	8773.07	13.50	0.23	2.12	0.17	69.78	2.37
1992 Jun 3	1.92	8777.08	13.47	0.12	2.22	0.13	69.08	1.74
1992 Jun 6	0.64	8780.03	13.60	0.10	2.58	0.17	69.03	1.89
1992 Jun 7	1.21	8781.05	13.40	0.11	2.28	0.14	67.19	1.77
1992 Jun 8	0.90	8782.04	13.23	0.11	2.25	0.16	66.74	2.00
1992 Jun 9	15.23	8783.63	13.30	0.07	2.50	0.12	69.77	1.40
1992 Jun 10	1.85	8784.08	13.02	0.10	2.31	0.14	69.67	1.80
1992 Jun 13	23.32	8787.97	13.09	0.10	2.59	0.15	69.92	1.59
1992 Jun 14	1.33	8788.06	12.73	0.12	2.45	0.16	67.36	1.84
1992 Jun 15	0.28	8789.01	13.39	0.09	2.50	0.14	65.84	1.65
1992 Jun 22	13.16	8796.55	13.19	0.10	2.65	0.12	69.23	1.35
1992 Jun 23	1.65	8797.07	12.75	0.14	2.94	0.33	74.53	3.40
1992 Jun 30	23.53	8804.98	12.82	0.10	2.60	0.15	70.89	1.65

TABLE 4D

8 GHz Light Curve for 3C 279

Date	UT (hr)	Truncated Julian Date	F (Jy)	σ (Jy)	Polarization (%)	σ (%)	Position Angle	σ
1991 Jan 19	11.22	8276.47	11.82	0.12	4.40	0.18	99°.55	1°.21
1991 Feb 6	9.95	8292.41	11.72	0.12	4.41	0.18	98.85	0.97
1991 Feb 13	10.16	8299.42	11.78	0.12	4.60	0.15	93.61	1.06
1991 Feb 18	7.57	8304.32	...	...	4.65	0.18	92.76	1.10
1991 Feb 26	9.73	8312.41	11.96	0.12	4.76	0.15	95.90	0.90
1991 Mar 7	9.09	8323.38	11.48	0.17	4.00	0.56	96.66	2.97
1991 Mar 15	7.84	8331.33	11.75	0.12	4.43	0.14	94.93	1.06
1991 Mar 17	6.62	8333.28	11.96	0.29	4.34	0.18	96.19	1.30
1991 Mar 30	7.23	8346.30	11.68	0.10	4.69	0.14	93.24	0.84
1991 Apr 14	6.37	8361.27	12.39	0.31	4.20	0.19	96.44	2.06
1991 Apr 15	6.68	8362.28	11.57	0.30	4.05	0.22	94.50	1.89
1991 Apr 30	5.26	8377.22	11.86	0.20	3.66	0.18	92.00	1.34
1991 May 2	2.76	8379.11	11.84	0.14	3.80	0.16	92.78	1.58
1991 May 4	2.84	8381.12	11.91	0.13	3.70	0.15	90.65	1.21
1991 May 13	4.85	8390.20	11.60	0.12	3.58	0.46	93.20	3.32
1991 May 16	4.22	8393.18	11.75	0.11	3.47	0.18	92.66	1.79
1991 May 24	3.45	8401.14	11.77	0.10	3.40	0.21	90.42	2.30
1991 Jun 3	3.58	8411.15	11.68	0.09	3.26	0.17	92.51	1.66
1991 Jun 18	2.56	8426.11	11.82	0.11	2.77	0.16	93.09	1.66
1991 Jun 24	1.40	9432.06	11.74	0.15	2.68	0.17	93.90	1.80
1991 Jul 3	22.38	8441.93	11.60	0.14	2.62	0.45	94.75	2.68
1991 Jul 5	23.82	8443.99	11.64	0.16	2.35	0.19	89.98	2.39
1991 Jul 18	23.34	8456.97	11.95	0.10	1.85	0.16	86.25	3.56
1991 Jul 30	23.18	8468.97	11.99	0.13	1.39	0.19	92.48	4.43
1991 Aug 9	22.35	8478.93	12.09	0.15	1.76	0.15	95.57	2.46
1991 Aug 10	20.52	8479.85	12.54	0.12	1.34	0.21	94.33	4.54
1991 Aug 16	21.63	8485.90	12.04	0.23	1.29	0.25	90.37	4.40
1991 Aug 27	20.36	8496.85	12.23	0.23	1.07	0.20	85.49	7.41
1991 Sep 8	20.02	8508.83	12.36	0.19	1.73	0.19	99.63	4.19
1991 Sep 17	19.29	8517.80	12.69	0.10	2.14	0.21	100.87	2.23
1991 Oct 29	14.86	8559.62	12.43	0.10	2.60	0.16	106.44	1.80
1991 Nov 1	17.20	8562.72	12.33	0.16	2.68	0.47	101.68	7.02
1991 Nov 8	16.41	8569.68	12.29	0.13	2.27	0.16	105.21	1.99
1991 Nov 13	16.28	8574.68	12.47	0.14	2.97	0.20	98.43	2.66
1991 Nov 22	16.63	8583.69	12.30	0.13	2.48	0.16	106.37	1.96
1991 Nov 28	15.71	8589.65	12.19	0.19	2.73	0.17	106.63	1.82
1992 Jan 20	10.06	8642.42	12.28	0.18	...	...	...	...
1992 Feb 4	11.30	8656.47	12.62	0.36	...	...	...	...
1992 Feb 11	10.29	8663.43	12.33	0.15	3.27	0.37	102.51	3.82
1992 Feb 14	10.41	8666.43	12.02	0.21	3.56	0.25	102.24	1.81
1992 Feb 23	9.77	8675.41	12.26	0.16	3.35	0.58	93.97	4.52
1992 Feb 25	7.49	8677.31	12.14	0.24	...	...	...	...
1992 Mar 2	6.58	8684.27	12.29	0.13	3.57	0.43	90.38	5.96
1992 Mar 3	9.10	8685.38	12.20	0.18	3.25	0.33	97.27	3.63
1992 Mar 5	10.11	8687.42	11.66	0.29	4.54	0.51	95.87	4.16
1992 Mar 19	8.55	8701.36	11.13	0.12	...	...	...	...
1992 Apr 1	7.38	8714.31	11.91	0.12	3.78	0.53	95.51	2.31
1992 Apr 14	6.59	8727.27	...	...	3.19	0.33	86.16	3.66
1992 May 9	4.57	8752.19	11.79	0.14	3.76	0.17	92.25	2.13
1992 May 12	4.04	8755.17	11.72	0.17	3.61	0.26	88.93	1.70
1992 May 25	1.58	8768.07	...	...	4.34	0.32	81.45	4.35
1992 Jun 1	2.50	8775.10	11.91	0.12	3.64	0.19	93.62	1.19
1992 Jun 11	1.91	8785.08	11.79	0.10	3.42	0.14	92.39	1.23
1992 Jun 16	1.66	8790.07	12.17	0.18	3.32	0.15	92.58	1.60
1992 Jun 26	1.13	8800.05	11.90	0.15	3.23	0.19	89.23	1.64

other blazars detected by EGRET (Fichtel et al. 1994; Hartman 1994; von Montigny et al. 1995), taking into account the short variation timescales observed (Kniffen et al. 1993; Hartman et al. 1993; Mattox et al. 1993). In most of these, Compton upscattering of soft photons has been utilized for production of the γ-rays. The soft photons can originate as synchrotron emission from within the jet (the synchrotron self-Compton or SSC process; Jones, O'Dell, & Stein 1974, Jones 1979, Marscher 1980, Königl 1981, Ghisellini, Maraschi, & Treves 1985, Marscher & Gear 1985, Maraschi, Ghisellini, & Celotti 1992a, Bloom & Marscher 1992, 1993, Marscher & Bloom 1992, Ghisellini et al. 1992, Marscher, Gear, & Travis 1992, Zdziarski & Krolik 1993), directly from a nearby accretion disk (Dermer, Schlickeiser, & Mastichiadis 1992; Dermer & Schlickeiser 1992, 1993, 1994; Melia & Königl 1989; Coppi, Kartje, & Königl 1993), or from disk radiation reprocessed in, e.g., broad emission-line clouds (Blandford 1993; Sikora, Begelman, & Rees 1993, 1994; Blandford & Levinson 1995). We refer to these latter models, in which the scattered seed photons are nonsynchrotron in origin, as external Compton scattering (ECS) models.

Marscher (1980) and Ghisellini et al. (1985) have demonstrated that the basic shape of the multifrequency spectra of

TABLE 4E

4.8 GHz Light Curve for 3C 279

Date	UT (hr)	Truncated Julian Date	F (Jy)	σ (Jy)	Polarization (%)	σ (%)	Position Angle	σ
1991 Jan 2	13.57	8259.57	10.32	0.17	6.27	0.15	106°.03	0°.82
1991 Jan 15	11.08	8272.46	10.31	0.15	5.58	0.12	105.47	0.62
1991 Feb 4	11.02	8290.46	10.51	0.13	5.42	0.12	105.35	0.64
1991 Feb 11	8.94	8297.37	10.44	0.16	5.29	0.12	104.04	0.67
1991 Feb 12	9.77	8298.41	10.48	0.16	5.38	0.12	104.98	0.64
1991 Feb 28	8.62	8314.36	10.32	0.14	5.41	0.12	104.98	0.62
1991 Mar 9	7.97	8325.33	10.62	0.14	5.20	0.13	104.25	0.67
1991 Mar 18	7.69	8334.32	10.42	0.14	5.16	0.13	104.46	0.77
1991 Mar 20	6.90	8336.29	10.40	0.20	5.17	0.12	103.76	0.65
1991 Apr 2	5.97	8349.25	10.54	0.23	4.99	0.12	103.39	0.67
1991 Apr 19	5.46	8366.23	10.20	0.12	5.02	0.13	105.53	0.75
1991 Apr 22	4.19	8369.17	10.23	0.15	5.20	0.12	104.44	0.66
1991 May 5	4.09	8382.17	10.41	0.15	4.82	0.12	104.97	0.71
1991 May 7	4.51	8384.19	10.22	0.14	5.00	0.12	104.38	0.67
1991 May 15.....	3.53	8392.15	10.35	0.15	4.67	0.12	104.98	0.74
1991 May 23.....	2.52	8400.10	10.32	0.16	4.63	0.13	103.92	0.80
1991 May 26.....	1.54	8403.06	10.26	0.22	4.70	0.15	104.09	0.86
1991 May 29.....	2.59	84.06.11	10.17	0.16	4.64	0.13	105.13	0.79
1991 Jun 23	1.05	8431.04	10.46	0.16	4.24	0.13	104.00	0.87
1991 Jul 2	23.39	8440.97	10.30	0.14	4.18	0.16	103.90	1.12
1991 Jul 15.....	22.80	8453.95	10.25	0.14	4.17	0.19	102.67	1.55
1991 Jul 17.....	22.73	8455.95	10.26	0.18	3.89	0.13	104.07	1.03
1991 Jul 26.....	22.85	8464.95	10.46	0.14	3.93	0.11	103.51	0.83
1991 Jul 29.....	22.17	8467.92	10.86	0.32	3.74	0.15	103.63	0.96
1991 Aug 6.....	22.53	8475.94	10.06	0.12	3.88	0.12	103.45	0.85
1991 Aug 21	21.59	8490.90	10.36	0.12	3.75	0.12	103.36	0.89
1991 Aug 29	21.10	8498.88	10.14	0.25	4.00	0.12	105.00	0.83
1991 Sep 1	21.55	8501.90	10.34	0.14	3.78	0.12	102.03	0.90
1991 Nov 19	16.73	8580.70	10.50	0.14	4.79	0.12	105.39	0.69
1991 Nov 21	16.05	8582.67	10.34	0.14	4.82	0.12	106.07	0.70
1991 Nov 29	15.39	8590.64	...	...	5.02	0.15	105.35	0.83
1991 Dec 10	14.98	8601.62	10.46	0.12	4.97	0.12	106.16	0.68
1991 Dec 15	14.25	8606.59	10.24	0.08	5.14	0.13	105.04	0.70
1991 Dec 28	14.16	8619.59	10.57	0.12	5.41	0.11	104.88	0.59
1991 Dec 29	11.67	8620.49	10.51	0.17	5.55	0.12	103.09	0.60
1992 Jan 1	11.10	8623.46	10.59	0.25	5.84	0.14	101.68	0.58
1992 Jan 4	13.89	8626.58	10.40	0.09	5.43	0.11	104.66	0.60
1992 Jan 7	12.89	8629.54	10.29	0.12	5.38	0.11	103.81	0.60
1992 Jan 16	12.99	8638.54	10.61	0.13	5.42	0.12	103.70	0.61
1992 Feb 1	11.86	8653.49	10.43	0.11	5.14	0.11	102.75	0.62
1992 Feb 16	8.96	8668.37	10.41	0.21	5.20	0.12	100.84	0.62
1992 Feb 28	9.80	8680.41	10.48	0.11	4.98	0.12	99.61	0.67
1992 Mar 10	8.64	8692.36	...	...	4.59	0.24	99.68	1.45
1992 Mar 21	7.80	8703.32	10.27	0.11	4.99	0.12	98.69	0.68
1992 Mar 23	6.10	8705.25	10.31	0.11	5.06	0.14	99.46	0.71
1992 Apr 3	6.95	8716.29	10.36	0.12	4.93	0.12	99.31	0.70
1992 Apr 11	6.36	8724.27	...	...	4.56	0.12	100.12	0.78
1992 Apr 21	5.75	8734.24	10.18	0.18	5.18	0.12	98.42	0.68
1992 Apr 23	4.22	8736.18	10.41	0.15	5.04	0.12	98.69	0.65
1992 May 5	4.88	8748.20	10.31	0.16	4.98	0.12	98.49	0.70
1992 May 13.....	4.84	8756.20	10.20	0.11	5.27	0.12	97.76	0.64
1992 May 27.....	3.11	8770.13	10.37	0.13	5.09	0.12	97.82	0.65
1992 Jun 1	0.78	8775.03	10.45	0.25	5.07	0.12	97.69	0.64
1992 Jun 5	0.76	8779.03	10.40	0.23	5.22	0.12	98.18	0.63
1992 Jun 13	0.18	8787.01	10.34	0.20	5.12	0.12	98.96	0.63
1992 Jun 17	0.28	8791.01	10.32	0.17	5.17	0.12	99.00	0.63

blazars can be understood as SSC emission from a tapered relativistic jet that accelerates from its base to the site of the radio emission. Since the magnetic field and (in the absence of continuous particle acceleration) relativistic electron energies decrease with distance along the jet, the transverse and axial dimension of the emission region decrease with increasing frequency of emission. Maraschi, et al. (1992a) have calculated an approximate multi–wave band SSC spectrum expected according to such a model, and they reproduce the 3C 279 spectrum rather well.

Some proposed approaches require production of extremely relativistic particles. Examples are direct synchrotron radiation (Maraschi, Ghisellini, & Celotti 1992b), deceleration of ultrarelativistic beams (Melia & Königl 1989; Coppi et al. 1993), and proton-driven jets (Mannheim & Biermann 1992; Mannheim 1993; Coppi et al. 1993).

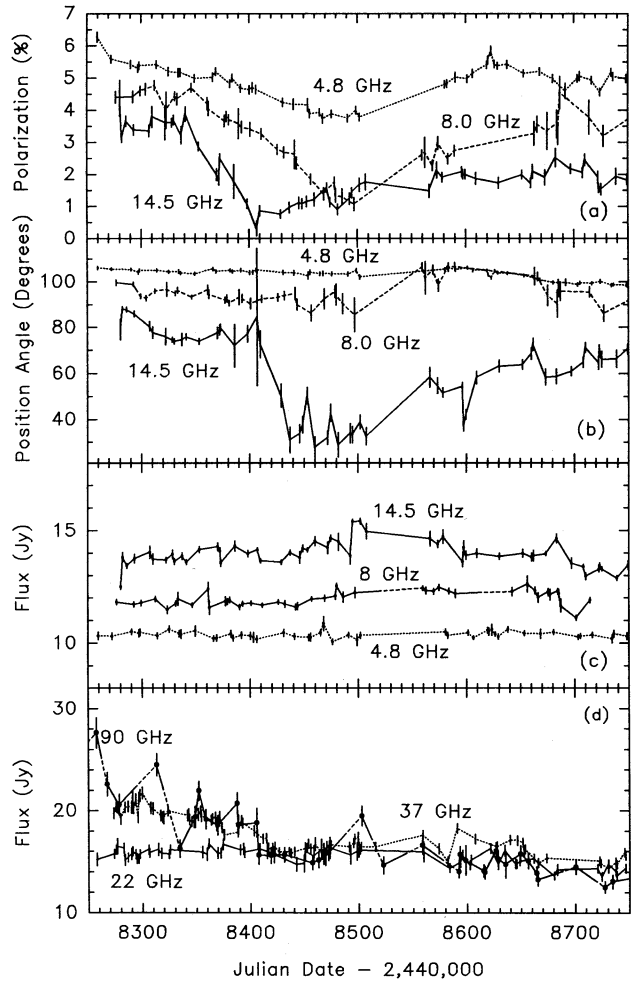

FIG. 3.—Radio light curves expanded vertically to permit easier inspection of variations in this range. In addition, histories of the University of Michigan polarization measurements at 4.85, 8.0, and 14.5 GHz are shown.

Extremely hot accretion disks have also been suggested (Eilek & Kafatos 1983; Becker, Kafatos, & Maisack 1994; Maisack, Becker, & Kafatos 1994), although it appears difficult to account for the TeV emission from Mrk 421 (Punch et al. 1992; Mohanty et al. 1993) in this manner.

If γ-ray variations are caused by changes in the number of relativistic electrons N_e in a jet, both the synchrotron (at optically thin frequencies) and γ-ray variations should be simultaneous in both the SSC and ECS models. In the ECS models, the variations of the synchrotron and γ-rays should be of the same magnitude, since each depends linearly upon N_e; but if the magnetic field also increases with increasing N_e, the magnitude of the γ-ray variation could be less than that of the synchrotron variation. In the SSC model, however, the ratio of self-Compton to synchrotron emission varies as N_e; hence, the γ-rays should show more pronounced variations than the synchrotron emission.

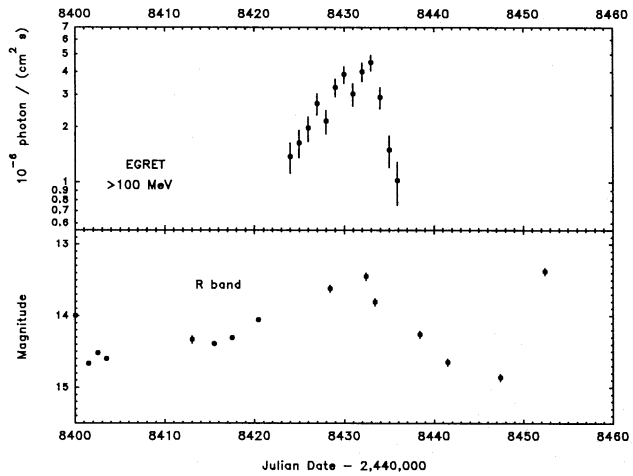

FIG. 4.—Magnification of the optical and γ-ray light curves during the 1991 June flare.

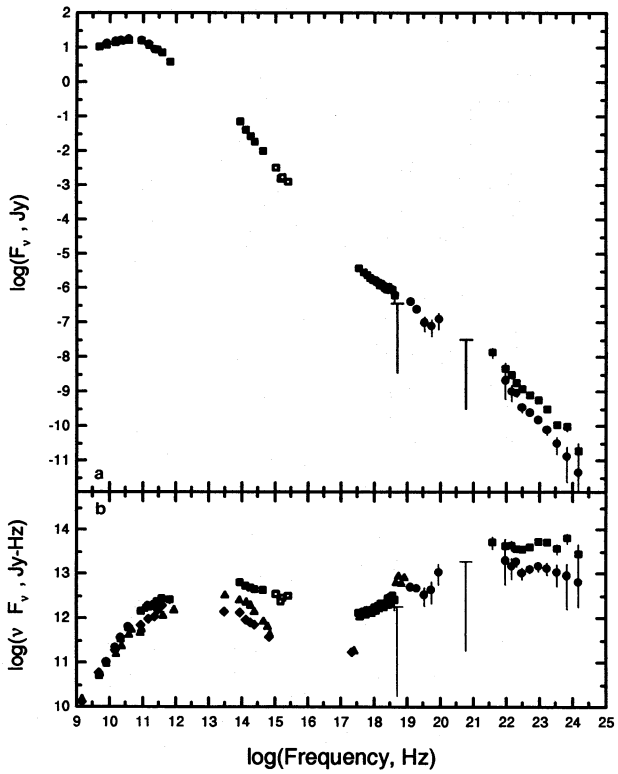

FIG. 5.—(*a*) Multiwavelength spectra during the 1991 June γ-ray flare (*squares*) and the 1991 October 3–17 EGRET observation (*circles*). At most frequencies, observations were impossible during October 3–17 because of the proximity of 3C 279 to the Sun; the radio points shown are averages of measurements just before and after the Sun exclusion interval. The scaled *IUE* points (see § 2.4) are shown as open squares. (*b*) The νF_ν spectrum corresponding to (*a*); for historical comparison, spectra are shown for 1984 (a quiet time [Brown et al. 1989]; *diamonds*) and 1988 (an extended flare [Makino et al. 1989]; *triangles*).

In the ECS models, γ-ray variations can also depend on variations in the seed photon flux, in which case the γ-ray variations should lag behind the variations of the directly observed photons. The synchrotron emission would then not be expected to show related variations. An increase in the bulk Lorentz factor could also produce large variations in the γ-ray/optical ratio within the ECS scenario. This ratio depends generally on observing angle, due to the different beaming patterns for synchrotron and external Compton-scattered radiation (Dermer, Sturner, & Schlickeiser 1995).

Which of the proposed γ-ray emission mechanisms dominates depends on the relative energy densities of the synchrotron photons and external (accretion disk or reprocessed disk) photons in the rest frame of the jet plasma, and on the relativistic proton/electron ratio in the jet. Since we do not know the size of the smallest synchrotron-emitting component of the jet, the size and scattering efficiency of the nonrelativistic scattering region,

TABLE 5

MULTIWAVELENGTH SPECTRA OF 3C 279

BAND	FREQUENCY	1991 JUNE		1991 SEPTEMBER–OCTOBER		SOURCE
		F_ν (Jy)	νF_ν (Jy-Hz)	F_ν (Jy)	νF_ν (Jy-Hz)	
4–10 GeV	1.48E24	(1.8 ± 1.2)E−11	(2.8 ± 1.8)E13	(4.3 ± 3.1)E−12	(6.3 ± 4.6)E12	EGRET
2–4 GeV	6.70E23	(9.6 ± 2.5)E−11	(6.4 ± 1.7)E13	(1.3 ± 1.1)E−11	(8.8 ± 7.2)E12	EGRET
1–2 GeV	3.35E23	(1.08 ± 0.25)E−10	(3.6 ± 0.8)E13	(3.1 ± 1.6)E−11	(1.0 ± 0.5)E13	EGRET
0.5–1 GeV	1.67E23	(3.1 ± 0.4)E−10	(5.1 ± 0.7)E13	(7.8 ± 2.3)E−11	(1.3 ± 0.4)E13	EGRET
300–500 MeV	9.25E22	(5.6 ± 0.6)E−10	(5.2 ± 0.6)E13	(1.5 ± 0.4)E−10	(1.4 ± 0.3)E13	EGRET
150–300 MeV	5.02E22	(7.9 ± 0.7)E−10	(4.0 ± 0.3)E13	(2.5 ± 0.5)E−10	(1.2 ± 0.2)E13	EGRET
100–150 MeV	2.94E22	(1.19 ± 0.13)E−9	(3.5 ± 0.4)E13	(3.5 ± 1.0)E−10	(1.0 ± 0.3)E13	EGRET
70–100 MeV	2.01E22	(1.76 ± 0.22)E−9	(3.5 ± 0.4)E13	(9.0 ± 2.0)E−10	(1.8 ± 0.4)E13	EGRET
50–70 MeV	1.42E22	(3.1 ± 0.7)E−9	(4.3 ± 1.0)E13	(1.0 ± 0.5)E−9	(1.4 ± 0.7)E13	EGRET
30–50 MeV	9.25E21	(4.5 ± 1.9)E−9	(4.2 ± 1.8)E13	(2.1 ± 1.5)E−9	(2.0 ± 1.4)E13	EGRET
8–30 MeV	3.75E21	(1.36 ± 0.42)E−8	(5.1 ± 1.6)E13	...	...	COMPTEL
0.75–8 MeV	5.92E20	<3.1E−8	<1.9E13	...	...	COMPTEL
370–600 keV	8.92E19	...	...	(1.2 ± 0.6)E−7	(1.1 ± 0.5)E13	OSSE
224–370 keV	5.42E19	...	...	(7.9 ± 4.0)E−8	(4.3 ± 2.2)E12	OSSE
138–224 keV	3.34E19	...	...	(9.8 ± 4.3)E−8	(3.3 ± 1.4)E12	OSSE
80–138 keV	1.94E19	...	...	(2.4 ± 0.3)E−7	(4.6 ± 0.5)E12	OSSE
51–80 keV	1.24E19	...	...	(3.9 ± 0.6)E−7	(4.8 ± 0.8)E12	OSSE
18.5–23.2 keV	4.99E18	<3.5E−7	<1.8E12	...	...	*Ginga*
16.2–18.5 keV	4.18E18	(6.1 ± 2.5)E−7	(2.5 ± 1.1)E12	...	...	*Ginga*
13.9–16.2 keV	3.62E18	(8.7 ± 1.7)E−7	(3.2 ± 0.6)E12	...	...	*Ginga*
12.7–13.9 keV	3.21E18	(9.2 ± 1.7)E−7	(2.9 ± 0.6)E12	...	...	*Ginga*
11.6–12.7 keV	2.93E18	(8.7 ± 1.4)E−7	(2.5 ± 0.4)E12	...	...	*Ginga*
10.4–11.6 keV	2.65E18	(1.05 ± 0.11)E−6	(2.8 ± 0.3)E12	...	...	*Ginga*
9.3–10.4 keV	2.37E18	(9.0 ± 0.9)E−7	(2.1 ± 0.2)E12	...	...	*Ginga*
8.1–9.3 keV	2.09E18	(9.9 ± 0.8)E−7	(2.1 ± 0.2)E12	...	...	*Ginga*
6.95–8.1 keV	1.81E18	(1.14 ± 0.07)E−6	(2.1 ± 0.13)E12	...	...	*Ginga*
6.37–6.95 keV	1.61E18	(1.30 ± 0.09)E−6	(2.08 ± 0.14)E12	...	...	*Ginga*
5.79–6.37 keV	1.47E18	(1.19 ± 0.08)E−6	(1.75 ± 0.12)E12	...	...	*Ginga*
5.21–5.79 keV	1.33E18	(1.40 ± 0.07)E−6	(1.86 ± 0.10)E12	...	...	*Ginga*
4.63–5.21 keV	1.19E18	(1.48 ± 0.07)E−6	(1.75 ± 0.08)E12	...	...	*Ginga*
4.05–4.63 keV	1.05E18	(1.65 ± 0.07)E−6	(1.72 ± 0.07)E12	...	...	*Ginga*
3.47–4.05 keV	9.04E17	(1.69 ± 0.07)E−6	(1.53 ± 0.06)E12	...	...	*Ginga*
2.89–3.47 keV	7.64E17	(1.90 ± 0.07)E−6	(1.45 ± 0.05)E12	...	...	*Ginga*
2.32–2.89 keV	6.24E17	(2.38 ± 0.08)E−6	(1.48 ± 0.05)E12	...	...	*Ginga*
1.74–2.32 keV	4.84E17	(2.84 ± 0.12)E−6	(1.38 ± 0.06)E12	...	...	*Ginga*
1.16–1.74 keV	3.41E17	(3.8 ± 0.4)E−6	(1.29 ± 0.12)E12	...	...	*Ginga*
	2.50E15	1.24E−3	3.1E12	...	...	*IUE*[a]
	1.67E15	1.69E−3	2.8E12	...	...	*IUE*[a]
	1.50E15	1.54E−3	2.3E12	...	...	*IUE*[a]
	1.07E15	3.2E−3	3.4E12	...	...	*IUE*[a]
R	4.29E14	(9.9 ± 0.5)E−3	(4.2 ± 0.2)E12	...	...	Balonek
J	2.40E14	(1.80 ± 0.01)E−2	(4.32 ± 0.02)E12	...	...	UKIRT
H	1.80E14	(2.60 ± 0.01)E−2	(4.68 ± 0.02)E12	...	...	UKIRT
K	1.30E14	(4.00 ± 0.03)E−2	(5.20 ± 0.04)E12	...	...	UKIRT
L'	8.70E13	(7.1 ± 0.04)E−2	(6.18 ± 0.35)E12	...	...	UKIRT
0.45 mm	6.60E11	3.8 ± 0.7	(2.5 ± 0.5)E12	...	...	JCMT
0.8 mm	3.80E11	7.1 ± 0.4	(2.71 ± 0.15)E12	...	...	JCMT
1.1 mm	2.70E11	8.5 ± 0.4	(2.29 ± 0.11)E12	...	...	JCMT
1.3 mm	2.30E11	8.5 ± 1.2	(2.0 ± 0.3)E12	8.7 ± 1.2	(2.0 ± 0.3)E12	JCMT
2.0 mm	1.50E11	11.5 ± 0.6	(1.73 ± 0.09)E12	12.3 ± 0.8	(1.85 ± 0.12)E12	JCMT
3.3 mm	9.00E10	15.7 ± 0.7	(1.41 ± 0.06)E12	14.3 ± 1.0	(1.29 ± 0.09)E12	SEST
8 mm	3.70E10	15.9 ± 0.4	(5.90 ± 0.15)E11	17.0 ± 0.6	(6.3 ± 0.3)E11	Metsähovi
1.4 cm	2.20E10	15.4 ± 0.7	(3.38 ± 0.15)E11	16.0 ± 1.0	(3.5 ± 0.22)E11	Metsähovi
2.1 cm	1.44E10	13.6 ± 0.1	(1.97 ± 0.01)E11	14.8 ± 0.4	(2.15 ± 0.05)E11	Michigan
3.8 cm	8.00E9	11.7 ± 0.2	(9.39 ± 0.12)E10	12.6 ± 0.2	(1.00 ± 0.02)E11	Michigan
6.2 cm	4.80E9	10.5 ± 0.2	(5.02 ± 0.08)E10	...	...	Michigan

[a] Scaled values; see text.

or the distance of the γ-ray production site from the putative accretion disk, we cannot determine theoretically which source of seed photons dominates in 3C 279. Therefore, we must rely on the multifrequency spectrum and variability to eliminate or constrain specific models.

4.2. *Spectrum*

The 1991 June quasi-simultaneous multifrequency spectrum presented in Figure 5 is apparently quite smooth through the radio-IR region. Although there is a large gap between 10^{12} and $10^{13.5}$ Hz, other blazars with coverage in that range show no significant deviation from a smooth spectrum (e.g., Clegg et al. 1983). The continuity of the spectrum at lower frequencies and an X-ray spectrum that is flatter than the IR-spectrum can be modeled effectively within the framework of the SSC model. The similar spectral indices of the submillimeter and X-ray portion of the spectrum are consistent with this interpretation. The shape

of the spectrum indicates that a break must occur at roughly 10^{14} Hz, at the low-frequency edge of the near-IR data shown in Figure 5. This break presumably reflects a similar change in slope of the relativistic electron energy distribution.

Since the slope of the γ-ray spectrum below 10^{23} Hz is similar to that of the synchrotron spectrum below 10^{14} Hz, straightforward application of the SSC model requires that the electrons responsible for the scattering up to hard γ-ray energies have Lorentz factors as high as $(10^{23}/10^{14})^{1/2} \sim 3 \times 10^4$. As is shown in Figure 6, a self-consistent model with a uniform relativistically moving source is not possible: either the γ-ray spectrum falls off too rapidly at high energies, or the model overpredicts the optical flux. A more complex model that has been shown to explain the behavior of spectral variations at radio-IR frequencies involves a shock wave propagating outward along a relativistic jet (Marscher & Gear 1985; Marscher et al. 1992). However, our numerical simulation of such a scenario has demonstrated that a model for SSC emission from such a shock also has difficulties explaining the multifrequency spectrum, similar to but less severe than those faced by the uniform spherical model.

Thus, the basic SSC model does not provide a ready fit to the quasi-simultaneous spectrum of 3C 279 at the time of the 1991 June γ-ray flare. That basic model, however, does not include anisotropies of the emission as seen by electrons in the source. If the magnetic field is at least partially ordered, as may be the case if the shock has a very small effective thickness (from radiative losses; see Marscher & Gear 1985), it is possible for the observer to see a different synchrotron spectrum than do the electrons. The synchrotron emission varies as $(\sin\theta)^{\alpha+1}$ (where $F_\nu \propto \nu^{-\alpha}$), and the break frequency varies as $\sin\theta$, where θ is the angle between the magnetic field and the line of sight (after accounting for relativistic aberration in the observer's frame). If a substantial fraction of the magnetic field, after correction for aberration, is nearly parallel to the observer's line of sight (as might be expected for a jet pointing almost at the observer, with a magnetic field aligned parallel to the jet axis), the standard calculation (based on observed quantities) will predict lower intensity synchrotron radiation and a lower break frequency as seen by the scattering electrons. The result is that the SSC γ-ray spectrum can extend to higher photon energies and can have higher observed γ-ray fluxes than would be expected according to a calculation that does not take into account the field orientation. Figure 7 shows a model fit (possibly not unique) to the multifrequency spectrum for a jet observed nearly along the axis, and with a magnetic field component aligned nearly parallel to the line of sight. The model result shown in Figure 7 has been obtained from a self-consistent computer code (Travis & Marscher 1996) for a shock-in-jet model, with the jet containing an axial magnetic field overlain by a random magnetic field component. The model jet has a conical geometry with magnetic field varying as r^{-1} and density varying as r^{-2}, where r is the distance from the apex of the cone. A power-law energy spectrum of relativistic electrons is injected at in inner radius $r_{\rm min}$ and allowed to decay due to losses from adiabatic expansion, synchrotron radiation, and first-order inverse Compton scattering. The main component of the magnetic field is assumed to be uniform and aligned with the jet axis. A randomly oriented component is superimposed whose magnitude is 50% of the uniform component. The jet opening half-angle is 1°.5, the jet axis is inclined by 5° to the line of sight, and a Lorentz factor of 5 is assumed for the bulk motion in the jet. The model spectrum provides a fairly good fit to the multiwavelength spectrum, demonstrating that such a multi–wave band spectrum can indeed be fitted by synchrotron-self-Compton emission from a relativistic jet. The introduction of a weak shock wave to explain the time variations does not alter the shape of the spectrum significantly as long as the electrons are assumed to gain energy only quasi-adiabatically because of the compression of the shock.

Therefore, we conclude that SSC models that incorporate the gradients in physical parameters found in relativistic jets can reproduce the multiwavelength spectrum rather well. The model is constrained by the requirement that it reproduce the synchrotron spectrum, including the flattening at radio frequencies from self-absorption, as well as the X-ray and γ-ray spectrum simultaneously. The particular model shown in Figure 7 does not allow for in situ particle acceler-

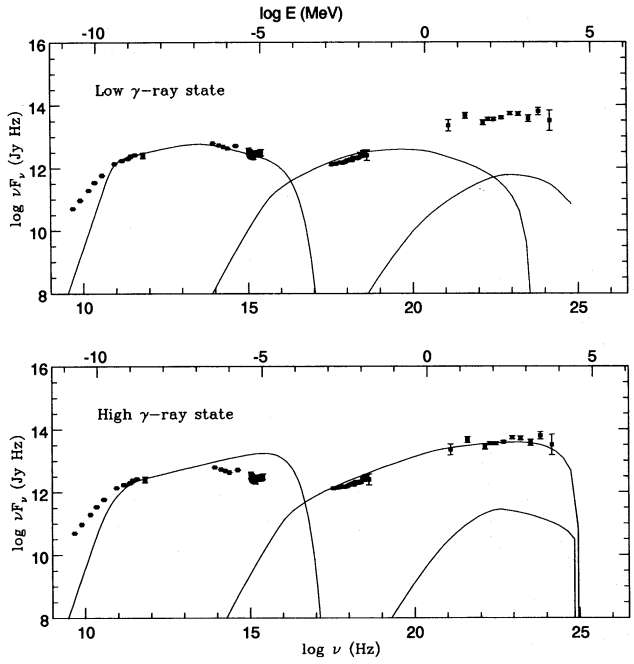

FIG. 6.—The best-fitting attempt to model numerically the 1991 June flare with SSC emission from a uniform, relativistic moving sphere.

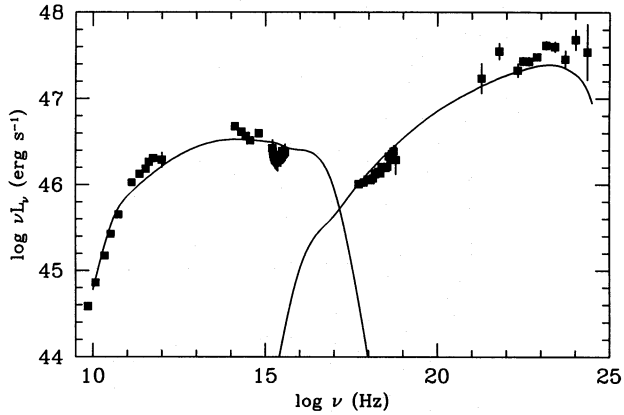

FIG. 7.—Comparison between the 1991 June flare spectrum and a numerical shock-in-jet SSC model which allows some portion of the magnetic field in the jet to be axially aligned. See text for details.

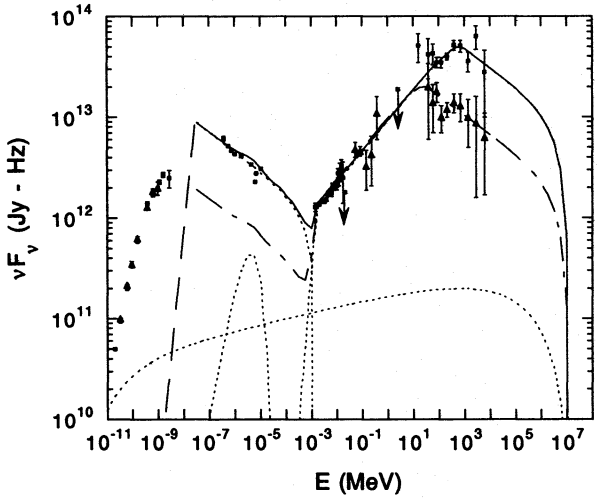

FIG. 8.—Solid and dot-dashed curves show fits to an external Compton scattering (ECS) model for the 1991 June (*squares*) and 1991 September–October (*triangles*) data, respectively. The synchrotron, synchrotron-self-Compton, disk, and external Compton scattering components are shown by the dotted curves for the fit to the 1991 June data. The long-dashed line indicates where the spectrum is optically thick to synchrotron self-absorption. See text for details and parameter values.

ation, bends in the jet, or other effects that probably occur in relativistic jets.

External Compton scattering models can also produce acceptable fits to the simultaneous multiwavelength spectra of 3C 279. In Figure 8 we show spectral calculations for the time-integrated spectrum of single-component plasma blobs moving with bulk Lorentz factor Γ in an external isotropic radiation field (see Dermer et al. 1995 for details of the model) In this simulation, $\Gamma = 10$, and electrons with Lorentz factors between 1 and 10^5 are isotropically injected in the comoving blob frame as a power-law spectrum with number index $p = 2.38$. The electrons cool by synchrotron radiation in a randomly oriented blob magnetic field of 1.7 G. The electrons also cool by scattering the synchrotron photons and the photons of an external radiation field, which are strongly aberrated in the comoving plasma frame due to the blob's relativistic motion. The external soft photon energy is chosen to be 5 eV, and the jet axis is assumed to be oriented at 3° with respect to the line of sight.

The solid curve in Figure 8 shows a fit to the 1991 June data. This spectrum is composed of four components, shown by the dotted curves. The narrow spectral component peaking near 5 eV represents the quasi-isotropic accretion-disk radiation which is spectrally broadened in the shape of a Shakura-Sunyaev (1973) outer blackbody spectrum. The very broad low-intensity spectral component is the beamed synchrotron self-Compton emission resulting from the Compton scattering of the synchrotron radiation which dominates the total spectrum below ~ 1 keV. The beamed external Compton scattering component is most important at higher energies. The external photons originate either directly from an accretion disk or after the accretion disk photons are scattered by surrounding gas and dust. The spectral break by a factor of 0.5, noted by Dermer & Schlickeiser (1993) and Sikora et al. (1993), results when the blob moves into a region in which the radiation field is less intense, so that electron cooling by external photons is no longer important. The spectra shown in Figure 8 represent the time-integrated emission from the injected electrons which cool by both synchrotron and Compton processes as the blob moves outward into a more dilute radiation field, which happens when the blob leaves the disk radiation field or the region containing scattering clouds. The dot-dashed curve in Figure 8 shows the spectral fit for the 1991 September–October data. All parameters for the two fits are the same except for the radial extent of the external scattering regions and the jet powers. The scattering regions are 2×10^{16} and 10^{17} cm in size for the 1991 June and 1991 September–October data, respectively, and the jet power is about 4 times as large in the former epoch as in the latter. The abrupt spectral break in the MeV portion of the spectrum would be smoothed out if the transition to a region with fewer external photons were more gradual.

An external Compton scattering model therefore provides a reasonable fit to multiwavelength spectra between infrared and γ energies. Below $\sim 10^{12}$ Hz, the blob spectrum is optically thick to synchrotron self-absorption, as indicated by the long-dashed line. Therefore, no attempt is made to model the radio emission which, in the ECS scenario, probably results from the superposition of self-absorbed components farther out along the jet. The magnetic field is stronger and the size of the blob is smaller in the EC model than in the SSC model, accounting for the difference in the magnitudes of the self-Compton components and self-absorption frequencies in the two models shown in Figures 7 and 8.

4.3. *Time Variation*

The timescale for substantial variation in γ-ray emission can be at least as short as a few days (Kniffen et al. 1993; Hartman et al. 1993; Mattox et al. 1993). This limits the line-of-sight dimension of the emitting region to $x < 10^{16}\delta/(1+z)$ cm, where z is the redshift and δ is the Doppler factor for relativistic bulk motion along the jet. A further constraint comes from the requirement that the region not be opaque to the γ-rays because of photon-photon pair production. We use equation (3) from Mattox et al. [1993; note that eqs. (2) and (3) of that paper must be divided by $(1+z)^4$ to correct an error] to determine that the 1991 June 3C 279 data require that the Doppler factor $\delta > 3.2$ in order for the optical depth to pair production by a ~ 3 GeV photon to be less than unity. (This assumes that the observed X-rays and γ-rays are produced in the same volume.)

The short timescale of variability is the main obstacle faced by the SSC model represented in Figure 7. The cross-sectional radius of the model jet at its narrowest point is 0.25 pc, or almost 8×10^{17} cm, whereas the Doppler factor at the jet axis is 8.4. Therefore, the region is 10 times the size of a region capable of varying substantially on a timescale of a few days. This is a fundamental problem for SSC models, one that can be solved either by adopting much higher Doppler factors or by assuming that the emission is located in a thin layer (such as a shock front; see Marscher & Gear 1985) viewed almost face-on. The short timescale of variability does not pose a difficulty for the single component ECS model. The fits shown in Figure 8 employ an accreting black hole of $10^8\ M_\odot$ and blobs with size ~ 100 gravitational radii, implying dynamical timescales shorter than 1 day.

Taken at face value, our observations indicate that the γ-ray flare in 1991 June was coincident with a short synchrotron flare observed in the R band. The amplitude of the γ-ray event appears to have been substantially higher, in

terms of fractional change, than that in the R band. The observations of Maraschi et al. (1994), which examine long-term multiwavelength variations of 3C 279, also suggest that the fractional variation in the γ-ray regime is greater than in the optical regime. This seems to favor the SSC model if it is assumed that only the electron number density N_e varies. If, however, the bulk Lorentz factor Γ changes (which in the case of long-term changes could be verified from subsequent VLBI observations), then ECS models can also explain the relative changes in the amplitudes of the components. A series of simultaneous observations would be necessary to discriminate between variations due to changes in N_e, Γ, or, as indicated by the modeling in Figure 8, the locations at which the nonthermal electrons are injected. In both the ECS and SSC models, short-timescale ($\lesssim$days) variations are probably due to quenching of the flare by inverse Compton energy losses of the electrons from intense soft-photon fields.

5. CONCLUSIONS

We have presented available simultaneous multiwavelength spectral data on 3C 279 for the periods 1991 June and 1991 September–October, in addition to light curves from 1991.0 to 1992.5 at a wide variety of frequencies. Although the γ-ray flux decreased by a factor of 4 between 1991 June and October (Kniffen et al. 1993), there was essentially no change in the 5–230 GHz range between those two epochs. No optical observations were possible during 1991 October; however, Maraschi et al. (1994) have previously demonstrated long-term correlation between the optical and γ-ray emission. Together, this suggests that the γ-ray and optical emission originate in separate regions from the site at which the radio emission is produced. During 1991 June, an R-band flare is seen to peak within about a day of the γ-flare peak. The short timescale of variation (1–2 days) suggests that the γ-ray emission is formed within a localized site rather than over the entire volume of an inhomogeneous emission region. For relativistic jet models, this implies that the γ-rays originate in the inner portions of the jet, close to its base, and probably in well-defined regions such as shocks or other locations with enhanced flow energy.

SSC and ECS models can provide reasonable fits to the simultaneous multiwavelength spectra. The γ-ray variation is explained in the SSC model by changes in the number of emitting electrons and in the ECS model by changes in the bulk Lorentz factor of outflowing plasma blobs or by changes in the location of the electron acceleration regions.

REFERENCES

Becker, P. A., Kafatos, M., & Maisack, M. 1994, ApJS, 90, 949
Blandford, R. D. 1993, in Compton Gamma Ray Observatory, ed. M. Friedlander, N. Gehrels, & D. Macomb (New York: AIP), 533
Blandford, R. D., & Levinson, A. 1995, ApJ, 441, 79
Bloom, S. D., & Marscher, A. P. 1992, in The Compton Observatory Science Workshop, ed. C. R. Shrader, N. Gehrels, & B. Dennis (NASA CP-3137), 339
———. 1993, in Compton Gamma Ray Observatory, ed. M. Friedlander, N. Gehrels, & D. Macomb (New York: AIP), 578
Bonnell, J. T., Vestrand, W. T., & Stacy, J. G. 1994, ApJ, 420, 545
Brown, L. M. J., et al. 1989, ApJ, 340, 129
Burstein, D., & Heiles, C. 1982, AJ, 87, 1165
Cameron, R. A., et al. 1992, in The Compton Observatory Science Workshop, ed. C. R. Shrader, N. Gehrels, & B. Dennis (NASA CP-3137), 3
Clegg, P. E., et al. 1983, ApJ, 273, 58
Coppi, P. S., Kartje, J. F., & Königl, A. 1993, in Compton Gamma Ray Observatory, ed. M. Friedlander, N. Gehrels, & D. Macomb (New York: AIP), 559
Dermer, C. D., & Schlickeiser, R. 1992, Science, 257, 1642
———. 1993, ApJ, 416, 458
———. 1994, ApJS, 90, 945
Dermer, C. D., Schlickeiser, R., & Mastichiadis, A. 1992, A&A, 256, L27
Dermer, C. D., Sturner, S. J., and Schlickeiser, R. 1995, in preparation
Diehl, R., et al. 1992, in The Compton Observatory Science Workshop, ed. C. R. Shrader, N. Gehrels, & B. Dennis (NASA CP-3137), 95
Duncan, W. D., et al. 1990, MNRAS, 243, 126
Eilek, J. A., & Kafatos, M. 1983, ApJ, 271, 804
Fichtel, C. E., et al. 1994, ApJS, 94, 551
Gear, W. K., et al. 1985, ApJ, 291, 511
Ghisellini, G., Maraschi, L., & Treves, A. 1985, A&A, 146, 204
Ghisellini, G., Padovani, P., Celotti, A., & Maraschi, L. 1992, in Testing the AGN Paradigm, ed. S. S. Holt, S. G. Neff, & C. M. Urry (New York: AIP), 398
Hartman, R. C. 1994, in The Gamma Ray Sky with CGRO and Sigma, ed. M. Signore, P. Salati, & G. Vedrenne (Dordrecht: Kluwer), 89
Hartman, R. C., et al. 1992, ApJ, 385, L1
———. 1993, ApJ, 407, L41
Hughes, P. A., Aller, H. D., & Aller, M. F. 1991, ApJ, 374, 57
Johnson, W. N., et al. 1993, ApJS, 86, 693
Jones, T. W. 1979, ApJ, 233, 796
Jones, T. W., O'Dell, S. L., & Stein, W. A. 1974, ApJ, 188, 353
Kanbach, G., et al. 1988, Space Sci. Rev., 49, 69
———. 1989, in Proc. Gamma-Ray Observatory Sci. Workshop, ed. W. N. Johnson (Greenbelt: NASA), 2-1
Königl, A. 1981, ApJ, 243, 700
Kniffen, D. A., et al. 1993, ApJ, 411, 133
Maisack, M., Becker, P. A., & Kafatos, M. 1994, ApJS, 92, 533
Makino, F., et al. 1989, ApJ, 347, L9
———. 1990, in Variability of Active Galactic Nuclei, ed. H. R. Miller & P. J. Wiita (Cambridge: Cambridge Univ. Press), 13
Makino, F., Fink, H. H., & Clavel. J. 1991, in Frontiers of X-Ray Astronomy, ed. Y. Tanaka & K. Koyama (Tokyo: Universal Academic Press), 543
Mannheim, K. 1993, A&A, 269, 67
Mannheim, K., & Biermann, P. L. 1992, A&A, 253, L21
Maraschi, L., Ghisellini, G., & Celotti, A. 1992a, ApJ, 397, L5
———. 1992b, in Testing the AGN Paradigm, ed. S. S. Holt, S. G. Neff, & C. M. Urry (New York: AIP), 439
Maraschi, L., et al. 1994, ApJ, 435, L91
Marscher, A. P. 1980, ApJ, 235, 386
Marscher, A. P., & Bloom, S. D. 1992, in The Compton Observatory Science Workshop, ed. C. R. Shrader, N. Gehrels, & B. Dennis (NASA CP-3137), 346
———. 1994, in The Second Compton Symposium, ed. C. Fichtel, N. Gehrels, & J. Norris (New York: AIP), 572
Marscher, A. P., & Gear, W. K. 1985, ApJ, 298, 114
Marscher, A. P., Gear, W. K., & Travis, J. P. 1992, in Variability of Blazars, ed. E. Valtaoja & M. Valtonen (Cambridge: Cambridge Univ. Press), 85
Matsuo, H., Matsumoto, T., & Murakami, H. 1989, PASJ, 41, 865
Mattox, J. R., et al. 1993, ApJ, 410, 609
Melia, F., & Königl, A. 1989, ApJ, 340, 162
Mohanty, G., et al. 1993, Proc. 23rd Int. Cosmic-Ray Conf. (Calgary), 440
Netzer, H., et al. 1996, MNRAS, in press
Punch, M., et al. 1992, Nature, 356, 447
Reich, W., et al. 1993, A&AS, 273, 65
Schönfelder, V., et al. 1993, ApJS, 86, 657
Seaton, M. J. 1979, MNRAS, 187, 73
Shakura, N., & Sunyaev, R. A. 1973, A&A, 24, 337
Sikora, M., Begelman, M. C., & Rees, M. J. 1993, in Compton Gamma Ray Observatory, ed. M. Friedlander, N. Gehrels, & D. Macomb (New York: AIP), 598
———. 1994, ApJ, 421, 153
Stevens, J. A., et al. 1994, ApJ, 437, 91
Teräsranta, H., et al. 1992, A&AS, 94, 121
Thompson, D. J., et al. 1993, ApJS, 86, 629
Travis, J. P., & Marscher, A. P., 1996, in preparation
Turner, M. J. L., et al. 1989, PASJ, 41, 345
von Montigny, C., et al. 1995, ApJ, 440, 525
Webb, J. R., Carini, M. T., Clements, S., Fajardo, S., Gombola, P. P., Leacock, R. J., Sadun, A. C., & Smith, A. G. 1990, AJ, 100, 1452
Williams, O. R., et al. 1995, A&A, 298, 33
Zdziarski, A. A., & Krolik, J. H. 1993, ApJ, 409, L33